LIMNOLOGY and OCEANOGRAPHY

ASLO

Limnol. Oceanogr. 67, 2022, 1343–1356

doi: 10.1002/lno.12086

Tight association between microbial eukaryote and giant virus communities in the Arctic Ocean

Jun Xia [1], **Sohiko Kameyama** [2], **Florian Prodinger** [1], **Takashi Yoshida** [3], **Kyoung-Ho Cho** [4], **Jinyoung Jung** [4], **Sung-Ho Kang** [4], **Eun-Jin Yang** [4], **Hiroyuki Ogata** [1], **Hisashi Endo** [1*]

[1]Institute for Chemical Research, Kyoto University, Kyoto, Japan
[2]Faculty of Environmental Earth Science, Hokkaido University, Sapporo, Japan
[3]Graduate School of Agriculture, Kyoto University, Kyoto, Japan
[4]Korea Polar Research Institute, Incheon, South Korea

Abstract

Viruses are important regulatory factors of the marine microbial community including microeukaryotes. However, little is known about their role in the northern Chukchi Sea in the Arctic basin, which has oligotrophic conditions in summer. To clarify the link between microbial eukaryotic communities and viruses as well as environmental conditions, we investigated the community structures of microeukaryotes (from 3 to144 μm and from 0.23 μm size bio-particles collected from seawater) and *Imitervirales* (from 0.23 μm size bio-particles collected from seawater), a dominant group of viruses infecting marine microeukaryotes. To the best of our knowledge, no study has investigated both *Imitervirales* and eukaryotic communities in the Arctic Ocean. Surface water samples were collected at 21 ocean stations located in the northeastern Chukchi Sea and an adjacent area outside the Beaufort Gyre (Adjacent Sea), and at two melt ponds on sea ice in the summer of 2018. At the ocean stations, nutrient concentrations were low in most of the locations, except the shelf in the adjacent sea. The community variations were significantly correlated between eukaryotes and *Imitervirales*, even within the northeastern Chukchi Sea characterized by relatively homogeneous environmental conditions. The association of the eukaryotic community with the viral community was stronger than that with geographical and physicochemical environmental factors. These results suggest that *Imitervirales* actively infect their hosts even in the cold and oligotrophic seawater in the Arctic Ocean.

The Arctic Ocean is the smallest, shallowest, and coldest ocean on earth. It covers several seas including the Chukchi Sea and the Beaufort Sea. Sea ice covers parts of the central area of the Arctic Ocean in summer and almost completely in winter due to the extreme seasonality of solar radiation in the polar region. Anthropogenic climate change is now accelerating and has had a strong impact on the Arctic Ocean (Stroeve et al. 2007; Lannuzel et al. 2020). Due to the ice-albedo feedback mechanism, sea ice has been melting faster compared to previous summers (Lindsay et al. 2012; Kashiwase et al. 2017). The highest surface air temperature during the past 120 years was recorded between 2014 and 2019 (http://www.arctic.noaa.gov/Report-Card). Upper sea water has also freshened as a result of the accelerating sea ice melting, and this situation is predicted to continue (Kwok and Cunningham 2010; Münchow 2016). In such changing environmental conditions, the way in which microorganisms form and alter their community structures through intricate interactions between them and with their surrounding environments is an important subject requiring further study.

Microbial eukaryotes play a fundamental role in the marine ecosystem (Worden et al. 2015). Integrated in the food web, they drive biogeochemical cycles by contributing to primary production (Falkowski et al. 1998; Field et al. 1998) and transferring fixed carbon to higher trophic levels (Sherr et al. 2007). Primary production in surface seawater of the Arctic Ocean observed by satellite remote sensing significantly increased from 1998 to 2018, presumably owing to the climate change-induced environmental changes such as sea ice melting and an increase in nutrient influx (Lewis et al. 2020). However, another study indicated that the abundance of nanophytoplankton (i.e., cell size of 2–20 μm) decreased from 2004 to 2008 in the Canada Basin

*Correspondence: endo@scl.kyoto-u.ac.jp

Additional Supporting Information may be found in the online version of this article.

Author Contribution Statement: J.X., S.K., H.O. and H.E. designed the study. S.K. collected the DNA samples. J.X., F.P. and T.Y. contributed biological experiments. J.X. and F.P. performed bioinformatics analyses. K-H.C., J.J., S-H.K., and E-J.Y., contributed to field sampling and the collection of physicochemical parameters. J.X. wrote the manuscript, which was edited and approved by all authors.
[Correction added on 03 May 2022, after first online publication: The author contribution statement has been corrected.]

while that of picophytoplankton (0.2–2 μm) increased because of a decrease in nutrient concentrations (Li et al. 2009).

The first study on molecular biological characterization of the microbial eukaryotic community in the Arctic Ocean was published 16 years ago (Lovejoy et al. 2006). Since then, several groups have carried out molecular barcoding studies to investigate microbial eukaryotic communities in different areas of the Arctic Ocean such as the Beaufort Sea, Amundsen Gulf, central Arctic Ocean, and West Spitsbergen (Comeau et al. 2011; Kilias et al. 2014; Marquardt et al. 2016). Strong seasonality has been revealed through the annual data of 18S rDNA derived from arctic surface water samples, with dominant microbial eukaryotic groups being remarkably different between summer and winter (Marquardt et al. 2016). Composition of the microbial eukaryotic communities in the Arctic Ocean is also shown to vary across water masses and environments with different physicochemical parameters and nutrient concentrations (Thaler and Lovejoy 2013; Kilias et al. 2014). These results collectively suggest the importance of environmental conditions in shaping microeukaryote communities at large time and spatial scales.

Apart from their physicochemical properties, viruses are thought to be key effectors of the communities of their microbial hosts in marine ecosystems (Suttle 2007; Middelboe and Brussaard 2017). *Imitervirales*, which belong to the phylum *Nucleocytoviricota* (also known as nucleocytoplasmic large DNA viruses, NCLDVs) (Iyer et al. 2006), is an order of virus that includes the so-called giant viruses. *Imitervirales* represents the most dominant group of DNA viruses infecting diverse microbial eukaryotes in the ocean (Endo et al. 2020). A previous study showed a tight association between the community of NCLDVs and that of microbial eukaryotes based on a global metagenomic dataset (Endo et al. 2020). However, as this result was based on a global scale dataset, the observed link was expected from substantial differences in the eukaryotic hosts inhabiting geographically distant and environmentally distinct locations. Investigating such virus-host associations at smaller geographic and time scales can provide further insights into the possible regulatory role of viruses on the host community structure. However, such local studies are currently scarce for *Imitervirales* (or NCLDVs) (Sandaa et al. 2018; Prodinger et al. 2022), and to the best of our knowledge, no study has investigated both *Imitervirales* and eukaryotic communities in the Arctic Ocean. We reasoned that examining whether the two communities are associated with each other in geographically close locations with similar environmental conditions and in the same period would lead to a better understanding of the interactions between *Imitervirales* and microbial eukaryotes. If virions persistently remain in an environment for a long period of time, then we would not expect a strong association between *Imitervirales* and microbial eukaryotes. In contrast, if viruses actively infect various eukaryotes, then a strong eukaryote-viral association would emerge.

The Mantel test is a statistical method used to test the correlation between two distance or dissimilarity matrices (Mantel 1967). For ecological studies, the Mantel test and partial Mantel test (Smouse et al. 1986) have been widely used to evaluate associations between microbial communities including viruses and related factors across local and global spatial gradients (Angly et al. 2006; Endo et al. 2020). Using a co-occurrence network analysis is another approach to dissect associations between microorganisms based on similarities in their emerging patterns. An improved tool named FlashWeave (Tackmann et al. 2019) yields more reliable relationships than simple correlation-based methods by removing the indirect association, thus has been used to evaluate the interactions between viruses and their hosts (e.g., *Imitervirales* and microeukaryotes) (Meng et al. 2021; Prodinger et al. 2022). Therefore, interactions between viruses and microeukaryotes can be inferred from both variations of overall communities and those of individual taxonomic units.

In this study, we conducted a high spatial resolution sampling of microbial DNA from the surface water during a 2018 cruise with the Korean ice breaking research vessel (IBRV) Araon. We investigated the community structures of microeukaryotes and *Imitervirales* in the basin region of the Chukchi Sea (the northeastern Chukchi Sea) as well as in an adjacent sea outside the Beaufort Gyre and melt ponds. The surface water of the northeastern Chukchi Sea is characterized by the low salinity and nutrients under the influence of the Beaufort Gyre system, making it distinct from the adjacent sea. To gain insight into the interdependence of eukaryotic and *Imitervirales* communities, we analyzed their statistical relationships while controlling the effects of environmental and geographical characteristics in the two different environmental regimes (the "stable" northeastern Chukchi Sea and the "dynamic" adjacent sea) using the Mantel test and partial Mantel test. We further constructed co-occurrence networks to dig into the associations between eukaryotes and *Imitervirales* at the taxonomic unit level.

Materials

Sampling sites and processes

During the Arctic Ocean Cruise on Araon 2018 belonging to the Korean Polar Research Institute (KOPRI), surface water samples were collected (SBE32 carousel water sampler) at 21 stations from August 06 to 22, 2018. Seawater temperature and salinity at 2 m depth were measured in situ using the conductivity–temperature–depth (CTD) sensors. Samples for chlorophyll *a* (Chl *a*) and nutrients were also collected at 2 m depth with Niskin-bottles. The current velocity at 5 m depth was measured using a lowered acoustic Doppler current profiler (LADCP, Teledyne RDI 300 kHz) and processed using the LADCP software (https://www.ldeo.columbia.edu/~ant/LADCP/). The environmental parameters in the additional two melt pond stations were collected at 0-m depth without the current velocity data. Samples for Chl *a* were filtered using 47 mm GF/F filters (with a nominal pore size of 0.7 μm) and Chl *a* was then extracted using 90% acetone (Jung et al. 2021). Extracted Chl *a* was

measured using a fluorometer (Trilogy, Turner Designs) (Lee et al. 2016). For the nutrient analysis, a 50 mL seawater sample for each site was collected with a conical tube and stored at 4°C. The concentrations of nitrite, nitrate, ammonia, phosphate, and silicate were measured using a four-channel continuous auto-analyzer (QuAAtro, Seal Analytical) following the Joint Global Ocean Flux Study (JGOFS) protocols (Gordon et al. 1993). Nutrient concentrations under the detection limit and lower than 0.005 μmol L^{-1} were considered 0.

Seawater (1 L) for the DNA analysis was collected at a depth of 2 m with Niskin-bottles attached to a conductivity–temperature–depth profiler with carousel multiple sampling (CTD-CMS) system for all stations except at two closed melt ponds (500 mL, 0 m depth), where water samples were collected just below the surface using a bucket. Collected seawater was prefiltered with a 144 μm pore-size mesh to remove large particles (prewashed with ultrapure water). Two liters of sea water were separated into two replicates. These were, then, filtered through a 3 μm Millipore membrane filter with an air pump (< 0.03 MPa). For larger size fractions, the water was further filtered through a 0.2 μm Millipore membrane filter using the same method for smaller sized fraction. The membrane filters and transferred to 1.5 mL microtubes and then stored in −20°C on board. These were, then, transferred to the laboratory while being continuously stored at −20°C.

DNA extraction and purification

DNA extraction and purification were performed following studies by Endo et al. (2018)). Briefly, each membrane filter was thawed at room temperature and was placed into the 1.5 mL microtubes with glass beads and xanthogenate buffer. The cells in the filter were crushed using a bead-beater, and the mixture was incubated at 70°C for 60 min. Glass beads were removed from the mixture after centrifugation. Subsequently, 600 μL isopropanol was added to the supernatant and mixed. The precipitated DNA was purified with a NucleoSpin gDNA Clean-up Kit (Macherey-Nagel). Finally, the purified DNA was dissolved using a low Tris-ethylenediaminetetraacetic acid buffer and stored at −20°C.

Eukaryotic 18S gene amplification and purification

Eukaryotic 18S rRNA gene V4 region fragments were amplified from extracted DNA of both 3–144 and 0.2–3 μm fraction sizes. This was done using primers E572F (5′-CYGCGGTAAT TCCAGCTC-3′) and E1009R (5′-AYGGTATCTRATCRTCTTYG-3′) (Comeau et al. 2011) with attached Illumina MiSeq 300 PE overhang reverse adapters as described in Illumina metagenomic sequencing library preparation protocols.

A 12.5 μL 2x KAPA HiFi HotStart ReadyMix was mixed with a 5 μL 1 μmol L^{-1} amplicon PCR forward primer, 5 μL 1 μmol L^{-1} amplicon PCR reverse primer, and 2.5 μL diluted DNA samples (0.25 ng μL^{-1}), and the mixture was then added into a PCR tube (final volume 25 μL). The amplification was performed for each sample with the following temperature cycling condition: initial denaturation at 98°C for 30 s was followed by 30 cycles of denaturation at 98°C for 10 s, annealing at 55 °C for 30 s, and 72°C for 30 s. A final extension step was completed at 72°C for 5 min.

Amplicons were purified with magnetic beads (Agencourt AMPure XP beads, Beckman Coulter). The purified DNA was dissolved in 25 μL ultrapure water and stored at −20°C.

Imitervirales polB gene amplification and purification

Degenerated 82 *polB* primer pairs (MEGAPRIMER, Supplementary Table S3) were used to amplify the *polB* gene of *Imitervirales* from 0.2 μm membrane filter (size-fraction 0.2–3 μm) DNA samples (Li et al. 2018). This size fraction contains free-living viral particles of *Imitervirales*, which generally have relatively large particle size (the range is generally from 0.2 to 0.8 μm) compared to phages, but also includes particle-associated viruses as some of the host species were picoeukaryotes (e.g., chlorophytes and haptophytes). A previously optimized amplification method named "MP10" (Supplementary Table S4) was performed. Amplification protocols, materials, and temperature cycling conditions were the same as in a previous study (Prodinger et al. 2020).

After amplification, we merged all eight amplicons generated from the same DNA sample using ethanol precipitation (Prodinger et al. 2020). Finally, the DNA precipitation was air-dried for approximately 10 min and suspended in 25 μL ultrapure water. Gel (2% agarose) extraction was performed to remove unspecific amplification products. Gel electrophoresis was made by adding 2% agarose gel. The gel was, then, stained in 5000x diluted SYBR gold buffer for 12 min. Approximately 400–500 bp visible bands were cut from the gel. Both Promega's Wizard SV Gel and PCR Clean-Up System were used to perform gel extraction according to the manufacturer's protocol. DNA was dissolved in 25 μL ultrapure water and then stored at −20°C.

Index PCR, library construction, and sequencing

Index PCR was performed following the Illumina Miseq platform protocol. Produced amplicons of eukaryotes and *Imitervirales* were purified with magnetic beads (Agencourt AMPure XP beads, Beckman Coulter). Finally, the DNA was dissolved in 27.5 μL ultrapure water and stored at −20 °C for less than 24 h. Produced amplicons of 0.2–3 μm eukaryotes were purified using gel and was performed by Macrogen Corporation in Japan.

DNA concentration was measured using a Qubit HS (high-sensitive) Kit. Library was denatured following the standard MiSeq normalization method provided by Illumina. The MiSeq Reagent Kit v2 and NaOH were used for the library with final DNA concentration of 2 nM. Paired-end sequencing was performed on the MiSeq platform.

Sequence processing and bioinformatic analysis

Eukaryotic 18S sequences were processed with QIIME2 (version: 2019.10) (Bolyen et al. 2019). Furthermore, 260 bp of left pair reads and 220 bp of right pair reads were trimmed. DADA2 was

used to cut primer sequences, merging paired end reads, performing quality control, dereplication, chimera check, and Amplicon Sequence Variants (ASVs) generation (Callahan et al. 2016). Singleton ASVs were removed. Taxonomic annotation was done using QIIME2's vsearch (Rognes et al. 2016) plugin and the SILVA 132 small subunit with a 97% similarity database (Quast et al. 2013) based on 97% sequence identity. Dominant ASVs (reads percentage over 0.50% of each size fraction) were found using blastn against the National Centre for Biotechnology Information (NCBI) Reference RNA sequences dataset, and results that included detailed linage information with the highest identity value were selected.

For the *Imitervirales* sequences, MAPS2 (*Mimiviridae* Amplicon Processing System) was used for the sequence analysis (Prodinger et al. 2022). DADA2 was used to check and remove megaprimer sequences, merging, quality control, dereplication, chimera check, and non-singleton ASV output. The ASVs were aligned against the *Imitervirales polB* amino acid sequence database (Li et al. 2018). Nucleotide sequences were translated into amino acid sequences and then added to the reference alignment using mafft (version: 7.453, parameters: --thread 8 -quiet --6merpair --addfragments) (Katoh and Standley 2013). Sequences that were assigned to the *Imitervirales* were saved for further analysis, while other sequences were removed. Translated ASVs were placed onto the reference phylogenetic tree including, isolated and environmental PolB sequences of NCLDVs (Endo et al. 2020) using pplacer software (version: 1.1. alpha19) (Matsen et al. 2010). The reference tree was built based on 905 long (≥ 700 amino acid) PolB sequences obtained from the Ocean Microbial Reference Gene Catalog (OM-RGC.v2) (Salazar et al. 2019) and 67 known NCLDV PolB sequences using the Randomized Axelerated Maximum Likelihood (RAxML) program (Stamatakis 2006). *Imitervirales* ASVs were then assigned to the reference tree. The 662 *Imitervirales* leaves in the tree were classified into 13 *Imitervirales* clades that were manually defined in a previous publication (Prodinger et al. 2022). The phylogenetic tree was edited and produced by iTOL v5.7 (https://itol.embl.de/).

Ecological analysis

Community composition was evaluated based on the number of reads of each ASV in every sample. ASVs were then subsampled using the rarefy function ("vegan" package) in R (version 3.6.3). Relative abundance was represented by the fraction of each ASV reads in each sample. The Shannon diversity index of eukaryotic and *Imitervirales* communities was calculated using R ("vegan" package) based on the subsampled ASV table. ANOVA and Tukey post hoc tests were performed by R ("agricolae" package). The Composition and diversity bar charts with error bars of standard deviation were calculated using Microsoft Excel (version 16.41). The map of sampling stations, temperature-salinity (TS) diagram, heatmap of environmental factors, and Shannon diversity were generated by Ocean Data View (ODV, version 5.1.5) (Schlitzer, R., Ocean Data View, https://odv.awi.de, 2018). Biological correlation was performed using the distance-based redundancy analysis (dbRDA) function, using R ("vegan" package) based on Bray–Curtis dissimilarity. For the dbRDA ordination, ASV composition was normalized by Hellinger transformation using the decostand function. Spearman's rank correlation was performed using R (rcorr function). The *p* value was also calculated using R (rcorr function). ANOSIM with 9999 permutation was performed for a biological data grouping test. Results of the dbRDA were plotted using ggord with 95% confidence interval circle contained samples in different water types. A non-metric multidimensional scaling (NMDS) analysis of *Imitervirales* community was performed using R (monoMDS function) based on the Bray–Curtis dissimilarity matrix made with the subsampled ASV table.

A Mantel test and partial Mantel test (Mantel 1967; Smouse et al. 1986) based on Pearson's correlation coefficient were performed as previously described (Endo et al. 2020), for calculating the correlation among geographic distance, environmental variables (i.e., a distance matrix combining temperature, salinity, dissolved inorganic nitrogen [DIN, nitrate + nitrite +- ammonium nitrogen], phosphate, and silicate), as well as eukaryotic and *Imitervirales* communities, using R ("ade4" package) with permutations of 1000. The geographic distance between each sampling station was calculated using R ("geosphere" package) from latitude and longitude data. Every environmental variable was standardized between the ranges of 0–1 (minimum and maximum values varying between 0 and 1). The Euclidean distance of environmental factors and Bray–Curtis dissimilarity of subsampled relative abundances of eukaryotes and *Imitervirales* between sampling sites were calculated with R. All *p* values were adjusted by Holm's method (Holm 1979) using R's p.adjust function.

Co-occurrence network analysis of eukaryotic and *Imitervirales* ASVs was performed by FlashWeave (Tackmann et al. 2019) with the parameters for the command "learn_network" as follows: transposed = true, sensitive = true, heterogeneous = false, normalize = true, and alpha = 0.001. Prior to the analysis, ASVs observed less than three samples were removed from the abundance profiles. Among all significant pairs of ASVs, only "eukaryote-virus" pairs (edges) having positive correlation values were considered as significant virus-host interaction signals.

Data availability

The raw reads generated in this study were uploaded to SRA (Sequence Read Archive) database on NCBI website. The accession numbers are from SRR12981736 to SRR12981758 under project ID PRJNA674408 (3–144 μm eukaryotic 18S), from SRR12981654 to SRR12981676 under project ID PRJNA674418 (0.2–3 μm eukaryotic 18S) and from SRR12981759 to SRR12981780 under project ID PRJNA674422 (0.2–3 μm *Imitervirales polB*). Additional files with original data are available at the GenomeNet (https://www.genome.jp/ftp/db/community/MEGAPRIMER_papers/Xia_et_al_2021/).

Results

Water characteristics and environmental factors

Twenty-one oceanic sampling stations (surface seawater samples) were classified into two groups (depending on the geographical locations and the temperature-salinity (TS) diagram) as follows: the northeastern Chukchi Sea (in the regions of Chukchi Plateau and Canada basin) and the adjacent sea (Figs. 1 and S2).

From the measured physical parameters (Supplementary Table S1), temperature showed little difference among stations, but salinity showed relatively large differences (Supplementary Table S1, Fig. 2A,B). Sea surface temperature (SST) in the northeastern Chukchi Sea (−0.99°C on average) was slightly higher than in the adjacent sea (−1.11°C on average), and the salinity in the northeastern Chukchi Sea (27.98 psu on average) was substantially lower than the adjacent sea (30.05 psu on average). Sea ice coverage in each station ranged between 0% and 89.5% (Supplementary Table S1).

Concentrations of nutrients (ammonia nitrogen, nitrate + nitrite, phosphate, and silicate) as well as Chl *a* were measured at each location. Most of the sampled area was oligotrophic, while water conditions of three "bloom" sites (stations A13, A14, A15; Chl *a* concentration > 4 mg m^{-3}) in the adjacent sea presented high nutrient concentrations. The nutrient and Chl *a* concentrations for the bloom stations (on average: nitrate + nitrite: 1.17 μmol L^{-1}; phosphate: 1.02 μmol L^{-1}; silicate: 14.15 μmol L^{-1}; Chl *a*: 7.23 mg m^{-3}) were much higher than those in other stations (on average: nitrate + nitrite: 0.14 μmol L^{-1}; phosphate: 0.52 μmol L^{-1}; silicate: 0.01 μmol L^{-1}; Chl *a*: 0.17 mg m^{-3}). Ammonia concentration was relatively high at Sta. A13 (0.11 μmol L^{-1}), while it was less than 0.02 μmol L^{-1} in other stations.

Amplicon sequences

Sequence information and the number of ASVs are summarized in Supplementary Table S2. The number of ASVs from each sample before subsampling is provided in Supporting Information Fig. S1. For the 3–144 μm eukaryotic community, 45,588–214,775 reads obtained from individual samples were subsampled at the minimum number of reads across different samples (i.e., 45,588 reads), and then grouped into 107–390 eukaryotic 18S non-singleton ASVs with the mean proportion of raw reads analyzed being 37%. For the 0.2–3 μm eukaryotic community, subsampling was performed at 72,359 reads, which was grouped into 106–385 eukaryotic 18S ASVs. For the *Imitervirales* community, subsampling was also performed at 26,638 reads, which generated 244–525 *Imitervirales polB* ASVs per sample.

Composition and local diversity of eukaryotic and *Imitervirales* communities

We first investigated eukaryotic communities by excluding sequences from metazoa and fungi, because they have different lifestyles and ecological functions from protists. The community compositions were different between large (3–144 μm) and small (0.2–3 μm) size-fractions (Fig. 3A,B). Eukaryotic communities of the large size fraction were dominated by dinoflagellates (36.6%

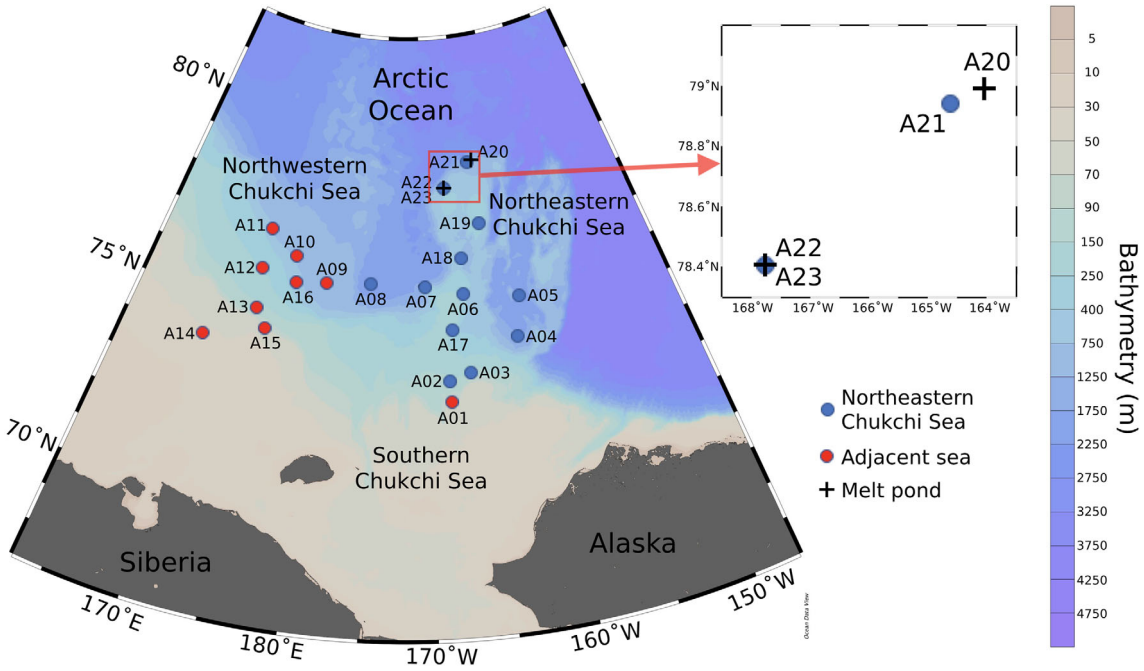

Fig. 1. Map of Arctic sampling stations. Symbol colors represent water types with different characteristics influenced by the current system in these areas. The color bar represents bathymetry. A22 and A23 were in the same location beside each other within 100 m.

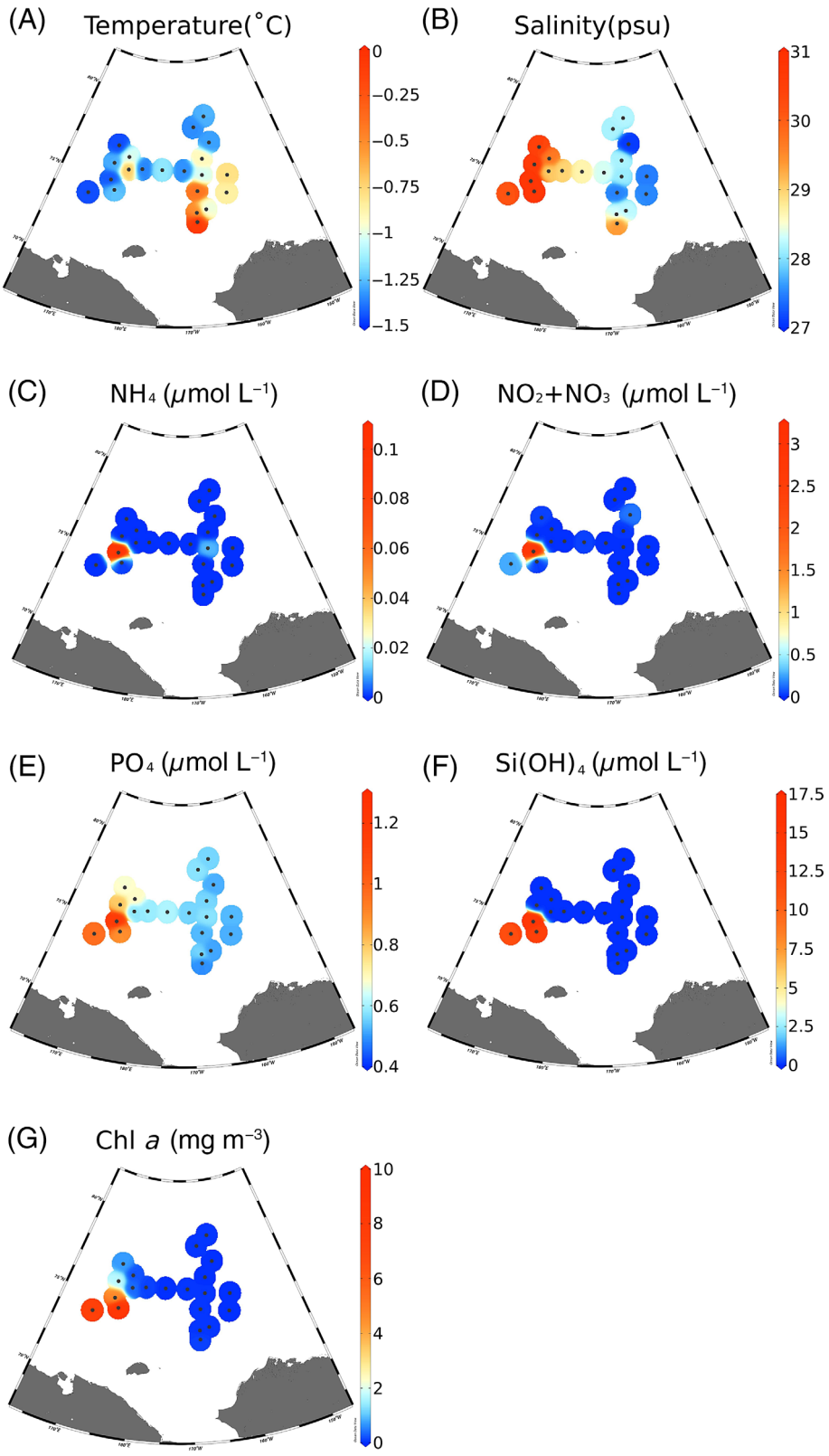

Fig. 2. Physical and chemical environmental variables among sampling sites: (**A**) temperature (°C); (**B**) salinity (psu); (**C**) NH_4 (μmol L^{-1}); (**D**) NO_2 and NO_3 (μmol L^{-1}); (**E**) PO_4 (μmol L^{-1}); (**F**) Si $(OH)_4$ (μmol L^{-1}); (**G**) Chl *a* (mg m^{-3}).

on average), diatoms (11.4%), and other marine alveolates (29.7%, include ciliates and protaveolata), while those of small size fraction were dominated by ciliates (28.5%), chlorophytes (19.8%), and picozoa (10.8%). In the large size fractions, lower proportion of dinoflagellates occurred in the adjacent sea sites than in the northeastern Chukchi Sea sites (ANOVA followed by Tukey post hoc tests, $p < 0.01$), especially in the three bloom samples (ANOVA followed by Tukey post hoc tests, $p < 0.05$). On the contrary, diatoms tended to be more abundant in the adjacent sea sites than in the northeastern Chukchi Sea sites (ANOVA followed by Tukey post hoc tests, $p < 0.01$). In the small size fraction, although the dominant ciliates had little difference among all the samples, chlorophytes showed a higher proportion in the adjacent sea bloom and the northeastern Chukchi Sea samples than in other samples from the adjacent sea sites (ANOVA followed by Tukey post hoc tests, $p < 0.01$). Another unique feature of the bloom sites was that there were almost no picozoa sequences in these samples, while the picozoa represented one of the abundant phyla in the other samples.

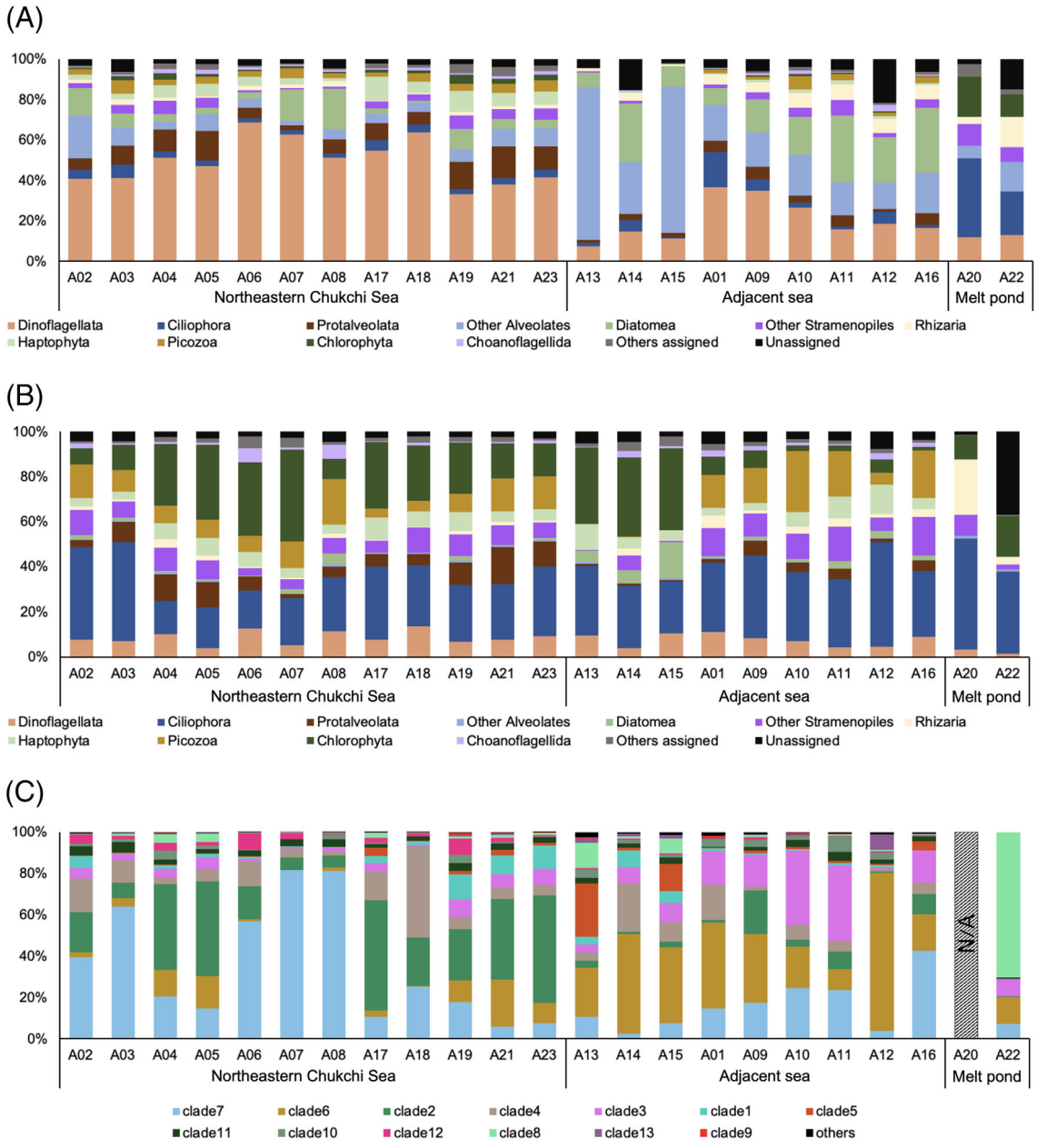

Fig. 3. Community compositions of eukaryotes and *Imitervirales*. Relative compositions of eukaryotes at the phylum level in (**A**) 3–144 μm fraction and (**B**) 0.23 μm fraction and (**C**) *Imitervirales* in the clade level. The color of each clade of the *Imitervirales* is the same as the phylogenetic tree (*see* Supporting Information Fig. S4). Fungi and Metazoa sequences were removed from eukaryotic sequences.

As for metazoa and fungal communities (*see* Supporting Information Fig. S3), copepods were the most dominant (20.0% on average) in the 3144 μm size fraction samples. As for the protist community, the most abundant ASVs (> 10% in at least one sample) in the large size fraction belonged to *Heterocapsa* (dinoflagellate), *Chytriodinium* (dinoflagellate), and *Gyrodinium* (dinoflagellate), while those in the small size fraction were *Micromonas* (chlorophyte), *Oligotrichia* (ciliate), *Chytriodinium* (dinoflagellate), *Phaeocystis* (haptophyte), *Chaetoceros* (diatom), and *Carteria* (chlorophyte) (Fig. 3A).

Imitervirales ASVs were mapped onto a larger set of *polB* sequences from the *Tara* Oceans dataset and classified into 13 clades (*see* Supporting Information Fig. S4). Clade 7 (28.6%) was the most abundant clade, followed by Clade 6 (20.2%), and Clade 2 (17.0%) (Fig. 3C). In the bloom sites, particularly high relative abundances were shown for Clades 5 and 6. In the other adjacent sea sites, Clade 3 which includes the OLPVs (Organic Lake phycodnavirus 1 and 2) showed higher proportions than in the northeastern Chukchi Sea. In the northeastern Chukchi Sea samples, Clade 2 showed high proportions (28.0% on average). A clear difference was found between the communities in the two aquatic habitats (sea water and melt pond water) for the eukaryotic and *Imitervirales* communities (Figs. 3A–C and S6). *Imitervirales* communities in the Arctic Ocean were clearly distinguished with those obtained from subtropical coastal sea water and hotspring samples using the same metabarcoding method (Li et al. 2019; Prodinger et al. 2020, 2022) (*see* Supporting Information Fig. S6). In the samples of this study, *Imitervirales* communities were classified into three groups: arctic seawater, arctic algae bloom-related seawater, and melt pond water (*see* Supporting Information Fig. S6). The sites in the northeastern Chukchi Sea and the adjacent sea shared 702 common *Imitervirales* ASVs, while 357 and 871 unique ASVs were detected in the northeastern Chukchi Sea and the adjacent sea sites, respectively (*see* Supporting Information Fig. S7A). It was also shown that 515 *Imitervirales* ASVs were shared between the bloom sites (A13, A14, and A15) and non-bloom sites (*see* Supporting Information Fig. S7B), while 319 and 1096 ASVs were unique to the bloom sites and non-bloom sites, respectively.

Shannon's diversity index was calculated for each community (*see* Supporting Information Fig. S5). Diversity of eukaryotic communities in the large size fraction showed the same variation trend as those in the small fraction among different samples. The three bloom sites in the adjacent sea had statistically lower diversity than others in both the large (ANOVA followed by Tukey post hoc tests, $p < 0.01$) and small eukaryotic communities (ANOVA followed by Tukey post hoc tests, $p < 0.01$). On average, the bloom sites had higher diversity of *Imitervirales* (4.34) than in other sites (3.83), although it was not statistically significant (ANOVA, $p = 0.068$) (*see* Supporting Information Fig. S5D).

Correlations with eukaryotic 18S community

Results from the dbRDA (Fig. 4) and Spearman's rank correlation (Supplementary Table S5) demonstrated that salinity and longitude were the two most significant variables in predicting Chl *a* biomass. The Chl *a* concentration also showed positive correlations with phosphate and silicate (phosphate: $r = 0.69$, $p < 0.01$; silicate: $r = 0.59$, $p < 0.01$). Current velocity had no measurable influence on community variation in different waters ($p > 0.05$). Eukaryotic as well as *Imitervirales* communities in the adjacent sea and northeastern Chukchi Sea were clearly separated from each other in a similar way as geographic distribution and TS diagram showed (*see* Supporting Information Fig. S2A).

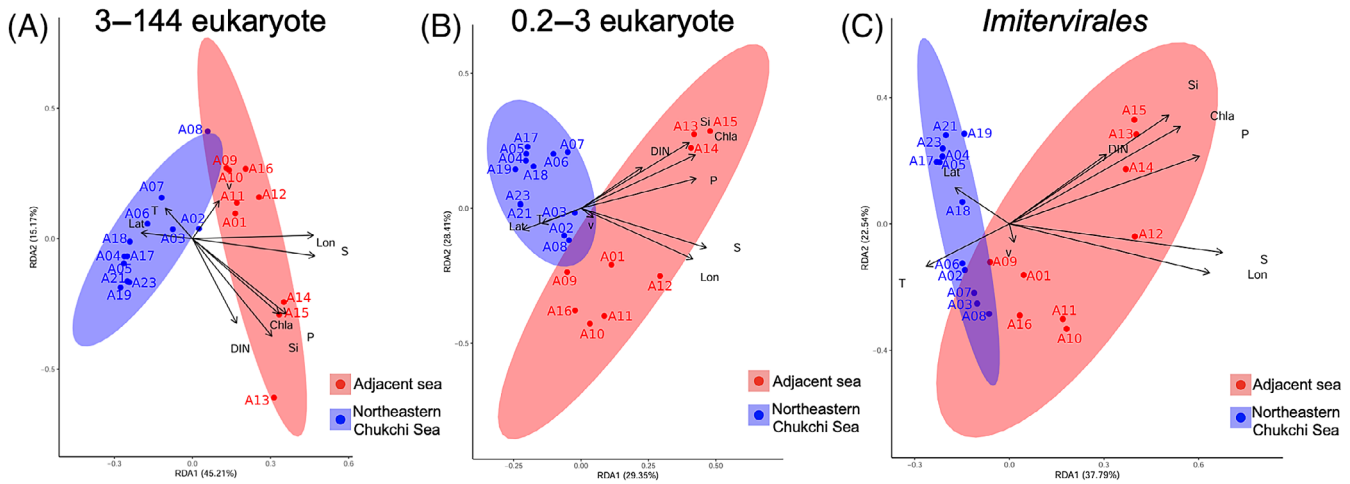

Fig. 4. Ordination diagram of the distance-based redundancy analysis (dbRDA): (**A**) 3–144 μm eukaryotic community based on 18S amplicon sequence variants (ASVs); (**B**) 0.2–3 μm eukaryotic community based on 18S ASVs; (**C**) *Imitervirales* community based on *polB* gene ASVs. Chl *a*, chlorophyll *a*; DIN, dissolved inorganic nitrogen (sum of ammonia, nitrite, and nitrate); Lat, latitude; Lon, longitude; P, phosphate; S, salinity; Si, silicate; T, temperature; v, current velocity.

According to the Mantel and partial Mantel tests, eukaryotic communities in both the large (3–144 μm) and small (0.2–3 μm) size fractions correlated significantly with *Imitervirales* communities in both the northeastern Chukchi Sea and adjacent sea sites ($q < 0.05$), even when the potential effects of spatial and environmental autocorrelations were removed (Table 1). Geographical distance was also a significant factor explaining the eukaryotic communities in the small fraction ($q < 0.05$), although no significant correlation was found for the large size fraction. For both the size fractions, environmental factors were significant explanatory variables for the eukaryotic communities among the adjacent sea sites, whereas no correlation was detected between environmental factors and eukaryotic communities in the northeastern Chukchi Sea sites. The Mantel test was also performed on the eukaryotic 18S communities and each environmental factor (Supplementary Tables S7 and S8). All the environmental factors in the northeastern Chukchi Sea sites were not significantly correlated with the eukaryotic 18S communities in the two size-fractions. In the adjacent sea sites, only phosphate and silicate were significantly correlated with the eukaryotic 18S communities.

To further examine the associations between *Imitervirales* and microeukaryotes suggested by the Mantel tests, we performed co-occurrence network analysis at the ASV level. We detected 315 and 292 edges (co-occurring signals) between *Imitervirales* and microeukaryotes for the large- and small-size fractions, respectively, in the network constructed based on the data of 21 sampling sites (Supplementary Table S11). Most of them (81% and 82% of microeukaryotes for the large- and small-size fractions, respectively) were positive edges (i.e., positive correlations). Among all the ASVs, 190 (37%) eukaryotic and 213 (27%) *Imitervirales* ASVs were included in the large-sized eukaryotes—*Imitervirales* positive correlations, while 166 (39%) eukaryotic and 199 (25%) *Imitervirales* ASVs were included in the small-sized eukaryotes—*Imitervirales* positive correlations. Abundant eukaryotic ASVs were also found in the networks (34 and 40 of top 50 eukaryotic ASVs for large- or small-sized eukaryotes, respectively). High numbers of positive edges and the inclusions of abundant ASVs in a network were reproduced when we divided the sites into the northeastern Chukchi Sea and adjacent sea (Supplementary Table S11).

Table 1. Mantel's *r* values between eukaryotic communities and geographical distance, environmental factor, or viral communities in the northeastern Chukchi Sea and adjacent sea. Environmental factor is defined as a combination of temperature, salinity, dissolved inorganic nitrogen ($NO_2 + NO_3 + NH_4$), phosphate, and silicate. The partial Mantel test was also applied to compare eukaryotic and *Imitervirales* communities while removing the effects of geographic distance and environmental factors. The Holm's-adjusted *p* values are listed in Supplementary Table S6.

	Northeastern Chukchi Sea ($n = 12$)	Adjacent sea ($n = 9$)
3144 μm eukaryote		
Geographic distance	0.30	0.34
Environmental factor	0.05	0.74**
Imitervirales	0.66***	0.70**
Imitervirales/geographic	0.63***	0.66**
Imitervirales/environmental	0.66***	0.61**
0.23 μm eukaryote		
Geographic distance	0.44**	0.30*
Environmental factor	0	0.63***
Imitervirales	0.65***	0.87***
Imitervirales/geographic	0.61***	0.86***
Imitervirales/environmental	0.65***	0.84***

*$q < 0.05$; **$q < 0.01$; ***$q < 0.001$.

Discussion

Basic environmental parameters and phytoplankton biomass

Oligotrophy is a common feature of surface sea water in the northeastern Chukchi Sea. Annual data (2008–2010) near the area indicated that concentration of nitrate plus nitrite in surface sea water of the study area was mostly depleted in the summer with values ranging between 0.01 and 0.1 μmol L^{-1} (Fujiwara et al. 2014). In our study, concentrations of nitrate plus nitrite also showed low values (≤ 0.14 μmol L^{-1}) except for some bloom samples in the adjacent sea (0.27–3.12 μmol L^{-1}) (Supplementary Table S1). The Chl *a* concentration, which is a proxy of phytoplankton biomass, was also low at the nutrient-depleted stations (0.02–1.70 mg m^{-3}) (Supplementary Table S1), suggesting the growth of phytoplankton was limited by nutrient availability (Ko et al. 2020). These values were also consistent with recent Chl *a* data at the corresponding area obtained from satellite (< 0.4 mg m^{-3}) (Lee et al. 2019a).

We separated seawater sampling sites into two groups, the northeastern Chukchi Sea and the adjacent sea, based on geographical locations. The grouping was also supported by the TS diagram in which the northeastern Chukchi Sea sites were characterized by lower salinity (*see* Supporting Information Fig. S2A). On one hand, the Beaufort Gyre, which influences water properties in the northeastern Chukchi Sea, is the greatest freshwater reservoir in the Arctic (Proshutinsky et al. 2019). On the other hands, samples having higher salinity were classified into the adjacent sea, because these locations would be more influenced by oceanic water masses and current regimes including Pacific water from the south and Atlantic water from the west (Jones 2001; Woodgate 2013). It is also shown that the main reason for an increase of salinity and nutrient concentrations (resulting from summer algal blooms) in the oligotrophic northeastern Chukchi Sea surface water is the intrusion of Atlantic cold saline water (Jung et al. 2021).

Community structures of microbial eukaryotes and *Imitervirales*

The eukaryotic communities were generally dominated by dinoflagellates, diatoms, and other alveolates in the large size fraction (3–144 μm) and by ciliates and chlorophytes in the small size fraction (0.2–3 μm) (Fig. 3A,B). Although the size of most ciliates is between 5 and 200 μm, the fragments from larger size bio-particles can pass through membrane filter as small as 3 μm. The dominance of these groups was roughly consistent with previous studies that examined the microbial eukaryotic community structures in the Arctic Ocean using molecular techniques (Lovejoy et al. 2006; Comeau et al. 2011; Marquardt et al. 2016; Xu et al. 2020) and the satellite ocean color remote sensing (Fujiwara et al. 2014; Lee et al. 2019b). Diagnostic pigment signatures have indicated that prasinophytes (Chlorophyta) were the dominant phytoplankton group in the northern Chukchi Sea, while diatoms and dinoflagellates were dominant in the southern Chukchi Sea (Fujiwara et al. 2014). Diatoms and chlorophytes are the common components of spring bloom in the Arctic Ocean (Von Quillfeldt 2000). In our study, the phytoplankton communities in the bloom sites were dominated by unclassified marine alveolates (45.9% relative abundance) and diatoms (13.5%) in larger size fraction (Fig. 3A). The representative sequence of the unclassified marine alveolate ASV was best hit to the dinoflagellate *Heterocapsa rotundata* in the NCBI Reference RNA sequences database (updated 07 July 2021) (100% sequence similarity). Although this dinoflagellate species has been detected typically in the temperate estuaries (Kyeong et al. 2006; Millette et al. 2015), it was also found to be common near the study area (Polyakova et al. 2021).

Unanticipatedly, high proportion of metazoan sequences were found in 3144 μm eukaryotic group (*see* Supporting Information Fig. S3). Most of them belong to copepods, which are predominant zooplankton in the Arctic Ocean (Kosobokova et al. 2011; Wang et al. 2019). However, body sizes of adult free-living copepods are usually above 200 μm, which cannot pass through the pre-filtration mesh. Although some of the copepod species (e.g., *Sphaeronellopsis monothrix*, 110 μm) are even smaller, they are the parasite of marine ostracods (Bowman and Kornicker 1967). It is reported that smaller eggs of copepods are produced by the adults in spring and summer, and some of these may float in the surface layer (Hirche and Niehoff 1996). Thus, one possible explanation for the dominance of metazoan sequences is the emergence of the larvae/eggs in the seawater.

We detected significant differences in the eukaryotic community between the northeastern Chukchi Sea and the adjacent sea for both size fractions by the dbRDA analysis (ANOSIM, $p < 0.01$) (Fig. 4A,B). In the large size fraction, communities of the northeastern Chukchi Sea sites were consistently dominated by dinoflagellates, whereas the relative abundance of dinoflagellates tended to be lower at the adjacent sea sites (Fig. 3A). In the small size fraction (Fig. 3B), a clear separation of microeukaryotic community was also detected by the dbRDA (Fig. 4B). We also evaluated eukaryotic communities from the two melt ponds on sea ice, which were located nearby the two northernmost seawater sites (Fig. 3C). The communities were largely distinct from seawater communities, most likely reflecting the difference in salinity between freshwater and seawater (Xu et al. 2020).

Besides eukaryotes, *Imitervirales* communities were analyzed in our study (Fig. 3C). Among *Imitervirales*, Clades 2, 6, and 7 were abundant lineages at most of the sampling sites (Figs. 3C and S5). Intriguingly, these three dominant clades do not include any reference species of *Imitervirales*. A previous study reported that the Arctic Ocean is a hot spot for endemic NCLDVs including *Imitervirales* (Endo et al. 2020); the dominant phylotypes detected in our study may support the high uniqueness of *Imitervirales* phylotypes in the study area. It is suggested that the geographical distribution of viruses follow those of the host species (Ibarbalz et al. 2019). The endemic feature is partly derived from the uniqueness of host eukaryotic species. Community compositions of *Imitervirales* were also differentiated between the northeastern Chukchi Sea and the adjacent sea stations by dbRDA analysis, as with the eukaryotic communities (Fig. 4C). Expectedly, NMDS analysis (*see* Supporting Information Fig. S6) clearly separated the *Imitervirales* communities in the arctic sites from those collected from coastal seawater and a hot spring in Japan, which were evaluated using the same MEGAPRIMER method. This separation would be due to the difference in host communities which are primarily determined by the environmental conditions.

Loose association between environmental variables and eukaryotic community

In this study, salinity was the primary factor used for dividing the sites between the northeastern Chukchi Sea and the adjacent sea (*see* Supporting Information Fig. S2A). Eukaryotic communities were also clearly separated between the northeastern Chukchi Sea and adjacent sea (Fig. 4A,B), with the compositions of eukaryotes being strongly influenced by the physical factors in the study area. Thus, we separately assessed the relationship between the eukaryotic community and environmental variables or *Imitervirales* community for the northeastern Chukchi Sea and the adjacent sea to eliminate possible spatial autocorrelation caused by the difference of eukaryotic communities among different water regimes.

In the adjacent sea sites, eukaryotic community was strongly correlated with environmental factor, but less correlated with geographical distance (Table 1). This suggests that the community was more affected by physicochemical environmental properties rather than dispersal events such as lateral advection among these sites. In fact, only the phosphate and silicate were significantly correlated with eukaryotic communities in the adjacent sea sites (Supplementary Tables S7 and S8). Environmental factors (Tables 1 and S6–S8) did not show any association with eukaryotic communities in the northeastern Chukchi Sea sites, whereas the effect of geographical distance was comparable to that detected in the adjacent sea sites. This indicates

that other factors may be more important in making up the eukaryotic communities in the Beaufort Sea basin. In our study, all the sampling sites in the northeastern Chukchi Sea were oligotrophic, and in some locations, the concentrations of nutrients were below the detection limit. Additionally, although temperature and salinity tend to be the key factors for microbial eukaryotic community structure and distribution in marine ecosystem (Sherr et al. 2007; Caron et al. 2016), these variables did not vary significantly among the northeastern Chukchi Sea sites. The low variation in environmental condition may cause the lack of correlation between environmental variables and the eukaryotic community.

Tight association between *Imitervirales* and the microbial eukaryotic community

In contrast to environmental variables, *Imitervirales* communities were consistently correlated with eukaryotic communities in both the northeastern Chukchi Sea and adjacent sea regions (Table 1). Notably, the correlation coefficients were rarely influenced by the geographical and environmental factors, suggesting that *Imitervirales* were associated with the eukaryotes in both types of water independently from environmental factors. This trend was most pronounced at the stations in the northeastern Chukchi Sea where environmental variables were relatively stable and had no correlation with eukaryotic community variations. Strong interplay between *Imitervirales* and microeukaryotes was further supported at the individual ASV level by the co-occurrence network analysis, which showed large numbers of positive associations between these entities in both the northeastern Chukchi Sea and the adjacent sea regions (Supplementary Table S11). Given the fact that *Imitervirales* are produced exclusively inside the eukaryotic hosts and most of the known *Imitervirales* are lytic (i.e., affect the host dynamics by causing mortality), local-scale variations of both *Imitervirales* and their host eukaryotes would have resulted from on-going viral infection. Our Mantel test and co-occurrence network analysis support the idea that the communities of *Imitervirales* and eukaryotes are actively interacting and co-varying without detectable influence from environmental conditions even in oligotrophic and homogeneous environments.

It has been suggested that biological interactions, such as predator–prey and symbiotic interactions, are responsible to determine community structure and the dynamics of microbes (Lima-Mendez et al. 2015; Chaffron et al. 2021). Additionally, viruses have been proposed as a key factor influencing the protist communities as they can impose top–down controls on their specific host populations (Nagasaki et al. 1994; Brussaard et al. 1996). Recent studies using Mantel statistics or co-occurrence network analysis indicated that *Imitervirales* are tightly associated with a variety of protist lineages at a global level (Endo et al. 2020; Meng et al. 2021), although only little of them have been isolated (Mihara et al. 2018). Our 18S rDNA barcoding revealed that chlorophytes and haptophytes, both of which are known host lineages of *Imitervirales*, were major protists in the small-size fraction. Although the dominating clades in the large-sized eukaryotic communities such as dinoflagellates, ciliophora, and diatoms have not yet been reported as host lineages, these groups were predicted to be the most closely linked host group for *Imitervirales* from a global scale network analysis (Meng et al. 2021). To date, some diatoms are known to be infected by smaller ssDNA and ssRNA viruses (Toyoda et al. 2012), and a dinoflagellate *Heterocapsa circularisquama* can be infected by ssRNA viruses and viruses of *Asfarviridae*, another clade of NCLDV (undefined Nagasaki et al. 2006). Therefore, the observed correlations between community variations would be the results of a large number of unknown virus–host interactions, including the viruses other than NCLDVs, and it is impossible to verify each of these interactions with our present limited knowledge of the virus–host pairs. Considering the highest proportion of *Imitervirales* among NCLDVs in the global ocean and their potential role as a top-down factor on host populations, relative compositions of the host lineages may well result from the combination of a variety of specific infections of NCLDVs and other viruses.

In the Arctic Ocean, an increase in sea surface temperature and decrease in sea ice cover are progressing (Praetorius et al. 2018; Peng et al. 2020). These climate change is associated with the shift of eukaryotic community structure as well as the increase of biomass and the potential loss of biodiversity in the past decade (Li et al. 2009; Arrigo and van Dijken 2015), although another study suggests a decreasing tendency on biomass (Hill et al. 2013). Increased temperature may provide competitive advantage to small nanophytoplankton over larger phytoplankton, resulting in an increase in the contribution of small phytoplankton in the community (Hare et al. 2007; Li et al. 2009). Our study showed that the association with the *Imitervirales* community was generally higher for the small-sized plankton community than for the large-sized community, implying that the role of *Imitervirales* in structuring the eukaryotic community in the study area may become increasingly important in the future. However, it should be noted that virus–host interactions can be influenced by the environments, especially temperature (Demory et al. 2017).

References

Angly, F. E., and others. 2006. The marine viromes of four oceanic regions. PLoS Biol. **4**: 2121–2131. doi:10.1371/journal.pbio.0040368

Arrigo, K. R., and G. L. van Dijken. 2015. Continued increases in Arctic Ocean primary production. Prog. Oceanogr. **136**: 60–70. doi:10.1016/j.pocean.2015.05.002

Bolyen, E., and others. 2019. Reproducible, interactive, scalable and extensible microbiome data science using QIIME 2. Nat. Biotechnol. **37**: 852–857. doi:10.1038/s41587-019-0209-9

Bowman, T. E., and L. S. Kornicker. 1967. Two new crustaceans: The parasitic copepod *Sphaeronellopsis monothrix* (Choniostomatidae) and lts Myodocopid ostracod host *Parasterope pollex* (Cylindroleberidae) from the southern New England coast. Proc. U S Nat. Museum **123**: 1–28. doi:10.5479/si.00963801.123-3613.1

Brussaard, C. P. D., R. S. Kempers, A. J. Kop, R. Riegman, and M. Heldal. 1996. Virus-like particles in a summer bloom of *Emiliania huxleyi* in the North Sea. Aquat. Microb. Ecol. **10**: 105–113. doi:10.3354/ame010105

Callahan, B. J., P. J. McMurdie, M. J. Rosen, A. W. Han, A. J. A. Johnson, and S. P. Holmes. 2016. DADA2: High-resolution sample inference from Illumina amplicon data. Nat. Methods **13**: 581–583. doi:10.1038/nmeth.3869

Caron, D. A., and others. 2016. Probing the evolution, ecology and physiology of marine protists using transcriptomics. Nat. Rev. Microbiol. **15**: 6–20. doi:10.1038/nrmicro.2016.160

Chaffron, S., and others. 2021. Environmental vulnerability of the global ocean plankton community interactome. Sci. Adv. **7**: eabg1921. doi:10.1101/2020.11.09.375295

Comeau, A. M., W. K. W. Li, J. É. Tremblay, E. C. Carmack, and C. Lovejoy. 2011. Arctic Ocean microbial community structure before and after the 2007 record sea ice minimum. PLoS ONE **6**: e27492. doi:10.1371/journal.pone.0027492

Demory, D., and others. 2017. Temperature is a key factor in micromonas-virus interactions. ISME J. **11**: 601–612. doi:10.1038/ismej.2016.160

Endo, H., and others. 2020. Biogeography of marine giant viruses reveals their interplay with eukaryotes and ecological functions. Nature Ecol. Evol. **4**: 1639–1649. doi:10.1038/s41559-020-01288-w

Endo, H., H. Ogata, and K. Suzuki. 2018. Contrasting biogeography and diversity patterns between diatoms and haptophytes in the Central Pacific Ocean. Sci. Rep. **8**: 1–13. doi:10.1038/s41598-018-29039-9

Falkowski, P. G., R. T. Barber, and V. Smetacek. 1998. Biogeochemical controls and feedbacks on ocean primary production. Science **281**: 200–206. doi:10.1126/science.281.5374.200

Field, C. B., M. J. Behrenfeld, J. T. Randerson, and P. Falkowski. 1998. Primary production of the biosphere: Integrating terrestrial and oceanic components. Biochem. Soc. Trans. **281**: 237–240. doi:10.1042/bst0040954

Fujiwara, A., T. Hirawake, K. Suzuki, I. Imai, and S. I. Saitoh. 2014. Timing of sea ice retreat can alter phytoplankton community structure in the western Arctic Ocean. Biogeosciences **11**: 1705–1716. doi:10.5194/bg-11-1705-2014

Gordon, L. I., Jennings, J. C., Ross, A. A., & Krest, J. M. (1993). A suggested protocol for continuous flow automated analysis of seawater nutrients (phosphate, nitrate, nitrite and silicic acid) in the WOCE hydrographic. WOCE Operations Manual, Tech. Rpt. 93-1. WOCE Hydrographic Program Office. http://www.ioccp.org/images/06Nutrients/WOCE_nutrients-manual_1993.pdf

Hare, C. E., K. Leblanc, G. R. DiTullio, R. M. Kudela, Y. Zhang, P. A. Lee, S. Riseman, and D. A. Hutchins. 2007. Consequences of increased temperature and CO2 for phytoplankton community structure in the Bering Sea. Mar. Ecol. Prog. Ser. **352**: 9–16. doi:10.3354/meps07182

Hill, V. J., P. A. Matrai, E. Olson, S. Suttles, M. Steele, L. A. Codispoti, and R. C. Zimmerman. 2013. Synthesis of integrated primary production in the Arctic Ocean: II. In situ and remotely sensed estimates. Prog. Oceanogr. **110**: 107–125. doi:10.1016/j.pocean.2012.11.005

Hirche, H. J., and B. Niehoff. 1996. Reproduction of the Arctic copepod Calanus hyperboreus in the Greenland Sea-field and laboratory observations. Polar Biol. **16**: 209–219. doi:10.1007/BF02329209

Holm, S. (1979). A simple sequentially rejective multiple test procedure. Scand. J. Stat., **6**, 65–70. http://www.jstor.org/stable/4615733

Ibarbalz, F. M., N. Henry, F. Lombard, C. Bowler, L. Zinger, G. Busseni, and H. Byrne. 2019. Global trends in marine plankton diversity across kingdoms of life. Cell **179**: 1084–1097. doi:10.1016/j.cell.2019.10.008

Iyer, L. M., S. Balaji, E. V. Koonin, and L. Aravind. 2006. Evolutionary genomics of nucleo-cytoplasmic large DNA viruses. Virus Res. **117**: 156–184. doi:10.1016/j.virusres.2006.01.009

Jones, E. P. 2001. Circulation in the Arctic Ocean. Polar Res. **20**: 139–146. doi:10.3402/polar.v20i2.6510

Jung, J., and others. 2021. Atlantic-origin cold saline water intrusion and shoaling of the nutricline in the Pacific Arctic. Geophys. Res. Lett. **48**: 1–10. doi:10.1029/2020GL090907

Kashiwase, H., K. I. Ohshima, S. Nihashi, and H. Eicken. 2017. Evidence for ice-ocean albedo feedback in the Arctic Ocean shifting to a seasonal ice zone. Sci. Rep. **7**: 1–10. doi:10.1038/s41598-017-08467-z

Katoh, K., and D. M. Standley. 2013. MAFFT multiple sequence alignment software version 7: Improvements in performance and usability. Mol. Biol. Evol. **30**: 772–780. doi:10.1093/molbev/mst010

Kilias, E., G. Kattner, C. Wolf, S. Frickenhaus, and K. Metfies. 2014. A molecular survey of protist diversity through the Central Arctic Ocean. Polar Biol. **37**: 1271–1287. doi:10.1007/s00300-014-1519-5

Ko, E., and others. 2020. Effects of nitrogen limitation on phytoplankton physiology in the Western Arctic Ocean in summer. J. Geophys. Res. Oceans **25**: e2020JC016501. doi:10.1029/2020JC016501

Kosobokova, K. N., R. R. Hopcroft, and H. J. Hirche. 2011. Patterns of zooplankton diversity through the depths of the Arctic's central basins. Marine Biodiversity **41**: 29–50. doi:10.1007/s12526-010-0057-9

Kwok, R., and G. F. Cunningham. 2010. Contribution of melt in the Beaufort Sea to the decline in Arctic multiyear sea ice coverage: 1993-2009. Geophys. Res. Lett. **37**: 1–5. doi:10.1029/2010GL044678

Kyeong, A. S., J. J. Hae, S. Kim, H. K. Gwang, and H. K. Jung. 2006. Bacterivory by co-occurring red-tide algae, heterotrophic nanoflagellates, and ciliates. Mar. Ecol. Prog. Ser. **322**: 85–97. doi:10.3354/meps322085

Lannuzel, D., and others. 2020. The future of Arctic Sea-ice biogeochemistry and ice-associated ecosystems. Nature Clim. Change **10**: 983–992. doi:10.1038/s41558-020-00940-4

Lee, Y., E. J. Yang, J. Park, J. Jung, T. W. Kim, and S. H. Lee. 2016. Physical-biological coupling in the Amundsen Sea, Antarctica: Influence of physical factors on phytoplankton community structure and biomass. Deep Sea Res. Part 1 Oceanogr. Res. Pap. **117**: 51–60. doi:10.1016/j.dsr.2016.10.001

Lee, Y., J. O. Min, E. J. Yang, K. H. Cho, J. Jung, J. Park, J. K. Moon, and S. H. Kang. 2019*a*. Influence of sea ice concentration on phytoplankton community structure in the Chukchi and east Siberian seas, Pacific Arctic Ocean. Deep Sea Res. Part 1 Oceanogr. Res. Pap. **147**: 54–64. doi:10.1016/j.dsr.2019.04.001

Lee, J., and others. 2019*b*. Latitudinal distributions and controls of bacterial community composition during the summer of 2017 in Western Arctic surface waters (from the Bering Strait of bacterial community composition during the summer of 2017 in Western Arctic surface waters from the Bering Strait to the Chukchi borderland). Sci. Rep. **9**: 1–10. doi:10.1038/s41598-019-53427-4

Lewis, K. M., G. L. Van Dijken, and K. R. Arrigo. 2020. Changes in phytoplankton concentration now drive increased Arctic Ocean primary production. Science **369**: 198–202. doi:10.1126/science.aay8380

Li, W. K. W., F. A. McLaughlin, C. Lovejoy, and E. C. Carmack. 2009. Smallest algae thrive as the arctic ocean freshens. Science **326**: 539. doi:10.1126/science.1179798

Li, Y., P. Hingamp, H. Watai, H. Endo, T. Yoshida, and H. Ogata. 2018. Degenerate PCR primers to reveal the diversity of giant viruses in coastal waters. Viruses **10**: 1–16. doi:10.3390/v10090496

Li, Y., H. Endo, Y. Gotoh, H. Watai, N. Ogawa, R. Blanc-Mathieu, T. Yoshida, and H. Ogata. 2019. The earth is small for "leviathans": Long distance dispersal of giant viruses across aquatic environments. Microbes Environ. **34**: 334–339. doi:10.1264/jsme2.ME19037

Lima-Mendez, G., and others. 2015. Ocean plankton. Determinants of community structure in the global plankton interactome. Science **10**: 1–10. doi:10.1126/science.1262073

Lindsay, R., and others. 2012. Seasonal forecasts of Arctic Sea ice initialized with observations of ice thickness. Geophys. Res. Lett. **39**: 1–6. doi:10.1029/2012GL053576

Lovejoy, C., R. Massana, and C. Pedrós-Alió. 2006. Diversity and distribution of marine microbial eukaryotes in the Arctic ocean and adjacent seas. Appl. Environ. Microbiol. **72**: 3085–3095. doi:10.1128/AEM.72.5.3085-3095.2006

Mantel, N. 1967. The detection of disease clustering and a generalized regression approach. Nature **27**: 209–220. doi:10.1038/124844a0

Marquardt, M., A. Vader, E. I. Stübner, M. Reigstad, and T. M. Gabrielsen. 2016. Strong seasonality of marine microbial eukaryotes in a high-Arctic fjord (Isfjorden, in West Spitsbergen, Norway). Appl. Environ. Microbiol. **82**: 1868–1880. doi:10.1128/AEM.03208-15

Matsen, F. A., R. B. Kodner, and E. V. Armbrust. 2010. pplacer: Linear time maximum-likelihood and Bayesian phylogenetic placement of sequences onto a fixed reference tree. BMC Bioinform. **11**: 538. doi:10.1186/1471-2105-11-538

Meng, L., H. Endo, R. Blanc-Mathieu, S. Chaffron, R. Hernández-Velázquez, H. Kaneko, and H. Ogata. 2021. Quantitative assessment of nucleocytoplasmic large DNA virus and host interactions predicted by co-occurrence analyses. MSphere **6**: 1–18. doi:10.1128/msphere.01298-20

Middelboe, M., and C. P. D. Brussaard. 2017. Marine viruses: Key players in marine ecosystems. Viruses **9**: 1–6. doi:10.3390/v9100302

Mihara, T., H. Koyano, P. Hingamp, N. Grimsley, S. Goto, and H. Ogata. 2018. Taxon richness of "Megaviridae" exceeds those of bacteria and archaea in the ocean. Microbes Environ. **33**: 162–171. doi:10.1264/jsme2.ME17203

Millette, N. C., D. K. Stoecker, and J. J. Pierson. 2015. Top-down control by micro- and mesozooplankton on winter dinoflagellate blooms of *Heterocapsa rotundata*. Aquat. Microb. Ecol. **76**: 15–25. doi:10.3354/ame01763

Münchow, A. 2016. Volume and freshwater flux observations from Nares Strait to the west of Greenland at daily time scales from 2003 to 2009. J. Phys. Oceanogr. **46**: 141–157. doi:10.1175/JPO-D-15-0093.1

Nagasaki, K., M. Ando, S. Itakura, I. Imai, and Y. Ishida. 1994. Viral mortality in the final stage of Heterosigma akashiwo (Raphidophyceae) red tide. J. Plankton Res. **16**: 1595–1599. doi:10.1093/plankt/16.11.1595

Nagasaki, K., Y. Tomaru, Y. Shirai, Y. Takao, and H. Mizumoto. 2006. Dinoflagellate-infecting viruses. J. Mar. Biolog. Assoc. U.K. **86**: 469–474. doi:10.1017/S0025315406013361

Peng, H. T., C. Q. Ke, X. Shen, M. Li, and Z. D. Shao. 2020. Summer albedo variations in the Arctic Sea ice region from 1982 to 2015. Int. J. Climatol. **40**: 3008–3020. doi:10.1002/joc.6379

Polyakova, Y. I., I. M. Kryukova, F. M. Martynov, A. E. Novikhin, E. N. Abramova, H. Kassens, and J. Hölemann. 2021. Community structure and spatial distribution of phytoplankton in relation to hydrography in the Laptev Sea and the east Siberian Sea (autumn 2008). Polar Biol. **44**: 1229–1250. doi:10.1007/s00300-021-02873-w

Praetorius, S., M. Rugenstein, G. Persad, and K. Caldeira. 2018. Global and Arctic climate sensitivity enhanced by changes in North Pacific heat flux. Nat. Commun. **9**: 1–12. doi:10.1038/s41467-018-05337-8

Prodinger, F., and others. 2020. An optimized metabarcoding method for mimiviridae. Microorganisms **8**: 1–17. doi:10.3390/microorganisms8040506

Prodinger, F., and others. 2022. Year-round dynamics of amplicon sequence variant communities differ among eukaryotes, Mimiviridae, and prokaryotes in a coastal ecosystem. FEMS Microbiol. Ecol. **97**: fiab167. doi:10.1101/2021.02.02.429489

Proshutinsky, A., and others. 2019. Analysis of the Beaufort Gyre freshwater content in 2003–2018. J. Geophys. Res. Oceans **124**: 9658–9689. doi:10.1029/2019JC015281

Quast, C., E. Pruesse, P. Yilmaz, J. Gerken, T. Schweer, P. Yarza, J. Peplies, and F. O. Glöckner. 2013. The SILVA ribosomal RNA gene database project: Improved data processing and web-based tools. Nucleic Acids Res. **41**: 590–596. doi:10.1093/nar/gks1219

Rognes, T., T. Flouri, B. Nichols, C. Quince, and F. Mahé. 2016. VSEARCH: A versatile open source tool for metagenomics. PeerJ **2016**: 1–22. doi:10.7717/peerj.2584

Salazar, G., and others. 2019. Gene expression changes and community turnover differentially shape the Global Ocean Metatranscriptome. Cell **179**: 1068–1083.e21. doi:10.1016/j.cell.2019.10.014

Sandaa, R. A., J. E. Storesund, E. Olesin, M. L. Paulsen, A. Larsen, G. Bratbak, and J. L. Ray. 2018. Seasonality drives microbial community structure, shaping both eukaryotic and prokaryotic host–viral relationships in an arctic marine ecosystem. Viruses **10**: 1–22. doi:10.3390/v10120715

Sherr, B. F., E. B. Sherr, D. A. Caron, D. Vaulot, and A. Z. Worden. 2007. Oceanic protists. Oceanography **20**: 130–134. doi:10.5670/oceanog.2007.57

Smouse, P. E., J. C. Long, and R. R. Sokal. 1986. Multiple regression and correlation Mantel test of matrix correspondence. Syst. Zool. **35**: 627–632. doi:10.2307/2413122

Stamatakis, A. 2006. RAxML-VI-HPC: Maximum likelihood-based phylogenetic analyses with thousands of taxa and mixed models. Bioinformatics **22**: 2688–2690. doi:10.1093/bioinformatics/btl446

Stroeve, J., M. M. Holland, W. Meier, T. Scambos, and M. Serreze. 2007. Arctic Sea ice decline: Faster than forecast. Geophys. Res. Lett. **34**: 1–5. doi:10.1029/2007GL029703

Suttle, C. A. 2007. Marine viruses - major players in the global ecosystem. Nat. Rev. Microbiol. **5**: 801–812. doi:10.1038/nrmicro1750

Tackmann, J., J. F. Matias Rodrigues, and C. von Mering. 2019. Rapid inference of direct interactions in large-scale ecological networks from heterogeneous microbial sequencing data. Cell Syst. **9**: 286–296.e8. doi:10.1016/j.cels.2019.08.002

Thaler, M., and C. Lovejoy. 2013. Environmental selection of marine stramenopile clades in the Arctic Ocean and coastal waters. Polar Biol. **37**: 347–357. doi:10.1007/s00300-013-1435-0

Toyoda, K., K. Kimura, N. Hata, N. Nakayama, K. Nagasaki, and Y. Tomaru. 2012. Isolation and characterization of a single-stranded DNA virus infecting the marine planktonic diatom Chaetoceros sp. (strain TG07-C28). Plankton Benthos Res. **7**: 20–28. doi:10.3800/pbr.7.20

Von Quillfeldt, C. H. 2000. Common diatom species in Arctic spring blooms: Their distribution and abundance. Botanica Marina **43**: 499–516. doi:10.1515/BOT.2000.050

Wang, Y. G., L. C. Tseng, M. Lin, and J. S. Hwang. 2019. Vertical and geographic distribution of copepod communities at late summer in the Amerasian Basin, Arctic Ocean. PLoS ONE **14**: 1–23. doi:10.1371/journal.pone.0219319

Woodgate, R. 2013. Arctic Ocean circulation: Going around at the top of the world. Nature Educ. Knowl. **4**: 8. https://www.nature.com/scitable/knowledge/library/arctic-ocean-circulation-going-around-at-the-102811553/

Worden, A. Z., M. J. Follows, S. J. Giovannoni, S. Wilken, A. E. Zimmerman, and P. J. Keeling. 2015. Rethinking the marine carbon cycle: Factoring in the multifarious lifestyles of microbes. Science **347**: 735–748. doi:10.1126/science.1257594

Xu, D., and others. 2020. Contrasting community composition of active microbial eukaryotes in melt ponds and sea water of the Arctic Ocean revealed by high throughput sequencing. Front. Microbiol. **11**: 1170. doi:10.3389/fmicb.2020.01170

Acknowledgments

The authors would like to thank colleagues from Korea Polar Research Institute for the help of sampling and physicochemical parameter determination; Tatsuhiro Isozaki, Kento Tominaga, and Hiroaki Takebe from Laboratory of Marine Microbiology, Kyoto University, for helping with DNA sequencing and support of experiment. The authors would also like to thank the captain and crew of the IBRV Araon Cruise for their support during the cruise. This work was supported by JSPS/KAKENHI (nos. 18H02279 and 19H05667 to Hiroyuki Ogata, 17H03850 to Takashi Yoshida and Hiroyuki Ogata, and nos. 19K15895 and 19H04263 to Hisashi Endo), Scientific Research on Innovative Areas from the Ministry of Education, Culture, Science, Sports and Technology (MEXT) of Japan (nos. 16H06429, 16K21723, and 16H06437 to Hiroyuki Ogata), and the Collaborative Research Program of the Institute for Chemical Research, Kyoto University (grant numbers 2016-28 and 2019-35). This research was also supported by the project titled "Korea-Arctic Ocean Warming and Response of Ecosystem (K-AWARE, KOPRI, 1525011760)," funded by the Ministry of Oceans and Fisheries, Korea (Kyoung-Ho Cho, Jinyoung Jung, Eun-Jin Yang, and Sung-Ho Kang). Computational work was completed at the SuperComputer System, Institute for Chemical Research, Kyoto University.

Conflict of Interest

None declared.

Submitted 27 September 2021
Revised 01 March 2022
Accepted 30 March 2022

Associate editor: Elisa Schaum